Supporting Information

Synchronously coupling defect and heteroatoms-doped carbon constraint layer on cobalt sulfides toward boosted oxide electrolysis activities for highly energy-efficient micro-zinc-air batteries

Juanjuan Zhao[a,b], Hao Tan[c], Zhenfa Zi[b], Li Song[c], Haibo Hu[a]*, Haijun Zhang[d]*, Mingzai Wu[a]*

a. Key Laboratory of Structure and Functional Regulation of Hybrid Materials, Ministry of Education, Institute of Energy, Hefei Comprehensive National Science Center, Anhui University, Hefei 230601;

b. School of Physics and Materials Engineering, Hefei Normal University, Hefei, 230601, China;

c. National Synchrotron Radiation Laboratory, University of Science and Technology of China, Hefei, 230029, China;

d. School of Safety Science and Engineering, Civil Aviation University of China, Tianjin, 300300, P. R. China.

Email: wumz@ahu.edu.cn; haibohu@ahu.edu.cn; hjzhang_ahu@163.com.

Experimental Section

Synthesis precursor Co-MOF {$[H_2N(CH_3)_2]_4[Co_3(Hdpa)_2]\cdot 3DMF$}

According to the synthesis method in the literature[1]: the mixture of H_6dpa (48.4 mg, 0.10 mmol) [H_6dpa=3,4-di(3,5-dicarboxyphenyl) phthalic acid] and $Co(NO_3)_2\cdot 6H_2O$ (43.7 mg, 0.15 mmol) was dissolved in DMF (2.5 mL) [DMF=dimethylformamide] in a screw-capped vial. After two drops of HNO_3 and 1.0 mL of H_2O were added to the mixture, the vial was capped and placed in an oven at 110 ºC for 8 h. The resulting single crystals were washed to give the Co-MOF.

Preparation of and $Co_{1-x}S$@N/S-C and CoS@N/S-C, CoS, N/S-C

The 100 mg of obtained cobalt-MOF and 100 mg of sublimed sulfur were placed respectively in two porcelain boats, the porcelain boat containing sublimed sulfur was in the upstream of the tube furnace. Whereafter, the sample was heat treated at 600 °C for 2 h at a heating rate of 5 °C min^{-1} in N_2 atmosphere and then naturally cooled to room temperature. After the heat treatment, the black powder is obtained, marked as $Co_{1-x}S$@N/S-C. For comparison, the CoS@N/S-C was synthesized in the same process as $Co_{1-x}S$@N/S-C except that the mass of sublimed sulfur was reduced to 10 mg. The pure CoS is commercially available. The pure N/S co-doped carbon (N/S-C) was prepared by 0.5 mol hydrochloric acid to remove the $Co_{1-x}S$ nanoparticles of $Co_{1-x}S$@N/S-C.

Fabrication and test of liquid rechargeable Zn-air batteries (ZABs)

The liquid ZAB was assembled with Zn-plate served as the anode and catalyst-coated carbon cloth (1 cm^2) served as the air electrode, the mixed solution of 6 M KOH and 0.2 M Zn $(CH_2COO)_2$ as electrolyte. Typically, 10 mg of catalyst was fully dispersed in a solvent consisting of 700 μL DI water, 240 μL isopropanol, and 60 μL Nafion solution by sonication for 2 h. Then, 100 μL catalyst ink was dripped on 1 cm^2 carbon cloth to achieve a catalyst loading amount of 1 mg cm^{-2}. ZABs tests were measurand with LAND battery testing system (LAND-CT2001A, China). Both the discharge/charge current and corresponding power densities were standardized to the active area of air cathode electrode.

Synthesis of polyacrylamide-co-polyacrylic (PAM-co-PAA) acid solid polymer alkaline electrolyte

Based on previous related preparation methods in literature 1, the 0.05 g N, N'-methylenebis (acrylamide) (AR grade, Aladdin) and 0.05 mL N, N, N', N'-tetramethylethylenediamine (CP

grade, Aladdin) were added in a mixed solution of 4.5 g acrylamide (AM, AR grade, Aladdin), then, 5 mL acrylic acid (AA, AR grade, Aladdin) dissolved in 50 ml DI water subsequently. This mixture was stirred with a magnetic stirrer until the reactant was dissolved completely. After the mixture being deoxygen for 30 min with nitrogen gas, 0.01 g initiator ammonium persulfate (APS) was added and stirred rapidly for 10 s. Taking the homogeneous solution (1 ml) into a cubic container and heating at 60 °C for 3 h, the polyacrylamide-co-polyacrylic acid) (PAM-co-PAA) gel film was obtained. Finally, the as-obtained PAM-co-PAA gel film was dried in a oven for 12 h at 80 °C to remove the water, and then soaked in a 20 mL mixture solution of 6 M KOH and 0.2 M Zn $(CH_2COO)_2$ for 24 h to form the PAM-co-PAA solid polymer alkaline electrolyte.

Synthesis of the GaIn semi-liquid metal

According to the method designed in the previous article[2], the 0.8 g Nickel (Ni) powders were slowly added in the 8 g commercial GaIn liquid metal under agitating with a glass bar at 90 ℃ until the Ni powders dispersed completely. After natural cooling, the semi-liquid metal was obtained defined as GaIn-Ni.

Fabrication and test of the a flexible/stretched solid state micro-ZAB (F/SmZAB)

Based on our previous researchs, first, finger-shaped Zn-foil (thickness of 0.03 mm) and carbon cloth were fabricated by a homemade interdigital cutting-mould. Then the as-prepared electrocatalyst ink was coated on the finger-shaped carbon cloth (loading amount of 1 mg cm^{-2}). Subsequently, the as-obtained interdigital anode/cathode electrodes were deployed on a solid alkaline gel electrolyte film supported by a bottom silicone encapsulation layer. After that, a top silicone encapsulation layer with air holes was overlaid on the well-deployed interdigital anode/cathode electrodes and adhered firmly to the bottom silicone encapsulation layer with semicured silicone serving as glue. After fully curing of the semicured silicone with thermal treatment in an oven of 50 °C for 30 min, the solid state micro-ZAB is successfully prepared. The F/SmZAB consists of three micro-ZABs connected in series or parallel which is used the GaIn-Ni liquid metal with a wavy shape as the electronic circuit and the homemade silicone as encapsulation layer.

Materials and characterization

All reagents and solvents were commercially available and were used without further purification. In addition, the microstructure and phase composition of the as-obtained samples

were characterized by Field-emission scanning electron microscopy (FE-SEM, S-4800, Hitachi, Japan), Transmission electron microscopy (TEM, JEM-2100, JEOL, Japan), X-ray powder diffraction (XRD Bruker D8-ADVANCE) with an 18 kW advanced X-ray diffractometer with Cu Kα radiation (λ=1.54056 Å). XPS was conducted with a Mg Ka achromatic X-ray source. The valence state and electron distribution of the material were analyzed by the K edge XAFS test of Co. The test site was Beijing Synchrotron Radiation Facility (BSRF, Line 1W1B). The results were analyzed by ATHENA and AREMIS, where the absorption curves were normalized. EXAFS signal χ(k) was used to deduct the background signals in front and behind the edges. Fourier transform spectra were obtained weighted $k^3\chi(k)$ in the range of 3~12 $Å^{-1}$. Electron paramagnetic resonance spectroscopy (JES-FA200) was used to characterize the vacancy of the samples. The test conditions were as follows: temperature 140 K, Ar flow protection, microwave frequency range 9082~9086 MHz, micro power 0.998 mW.

Electrochemical characterizations

The catalyst ink was prepared by dispersing catalyst (10 mg) and 50 μL Nafion (DuPont) into 700 μL DI water and 250 μL isopropanol by sonication. The electrochemical activities (CV, ORR and OER) of the catalysts were tested in a standard three electrodes system on the electrochemical workstation (CHI 760E) in 0.1 M saturated KOH electrolyte at room temperature. The working electrode was a glassy carbon rotating disk electrode (diameter 5 mm) which drop casted with the catalyst ink to a loading amount of 0.2 mg cm^{-2}. The counter electrode was a platinum electrode, and a saturated calomel electrode (SCE) as a reference electrode. All potentials here are converted to a reversible hydrogen electrode (RHE) scale, $ERHE = E_{Ag/AgCl} + 0.059pH + E_{\theta Ag/AgCl}$. The catalytic performance toward the ORR was measured from -0.8 to 0.2 V (vs. Ag/AgCl). The catalytic activity for OER was evaluated from 0 to 1.0 V (vs. Ag/AgCl). In comparison, commercial 20 wt% Pt/C catalyst ink (for ORR) and the RuO_2 catalyst ink (for OER) were prepared using the same procedure. The cyclic voltammetry (CV) measurements were performed at 20 mV s^{-1} from -0.8 to 0 V (vs. Ag/AgCl) in O_2-saturated and N_2-saturated electrolyte, respectively. In order to test the electrochemical performances of the catalysts for ORR, the linear sweep voltammetry (LSV) carves were performed at a scanning rate of 5 mV s^{-1} from -0.8 V to 0.2 V (vs. Ag/AgCl) at different rotation rates (400~2500 rpm) in O_2-saturated electrolyte. Rotating ring-disk electrode (RRDE: Pine Research Instrument, USA) voltammogram measurements for the calculation of the ORR electron transfer number were conducted on an RRDE configuration with a 320 μm gap Pt ring electrode. The electron transfer numbers (n) and peroxide yield

(HO_2^- %) can be obtained from the RRDE curve using the Eqs, respectively.

$$n = 4 \times \frac{I_d}{I_d + I_r/N} \qquad HO_2^- \% = 200 \frac{I_r/N}{I_d + I_r/N}$$

where I_d is the disk current, I_r is the ring current and N is the current collection efficiency of the Pt ring which was determined to be 0.37. Electrochemical impedance spectroscopy (EIS) measurements were evaluated with the frequency range from 100 kHz to 0.01 Hz.

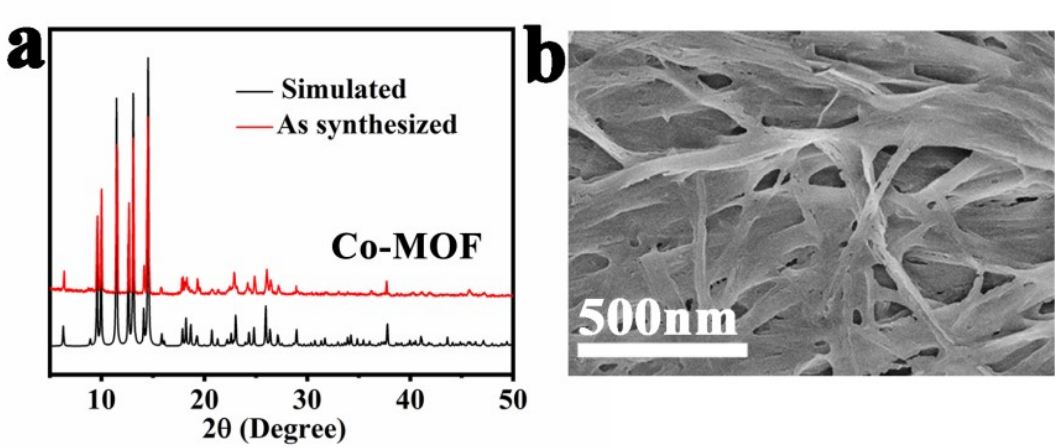

Figure S1. (a) The XRD patterns of the Co-MOF and (b) the corresponding SEM image of it.

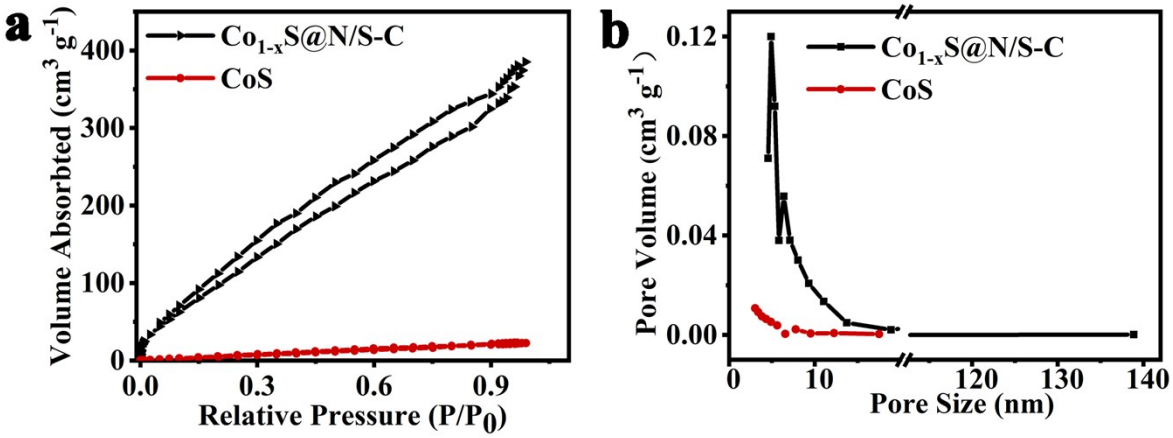

Figure S2. (a) N_2 adsorption-desorption isotherms and (b) BJH pore-size distribution of the $Co_{1-x}S$@N/S-C and CoS.

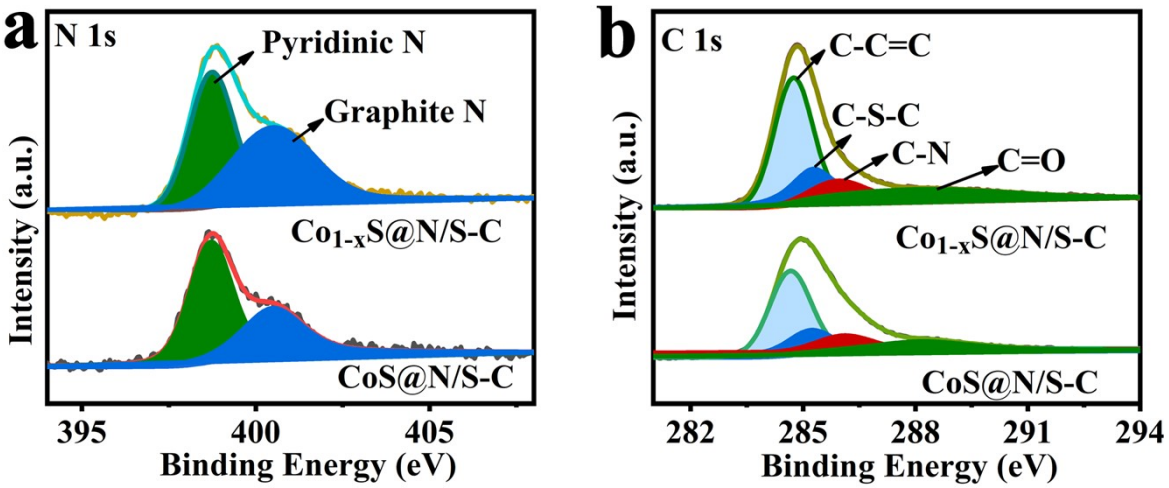

Figure S3. The XPS high-resolution spectra of the (a) N 1s and (b) C 1s for $Co_{1-x}S$@N/S-C, CoS@N/S-C.

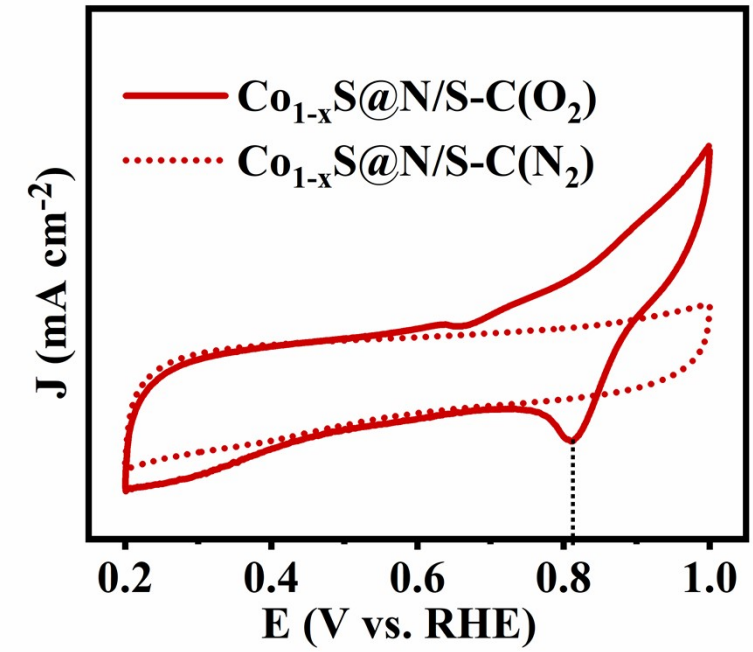

Figure S4. CVs of the $Co_{1-x}S$@N/S-C in N_2 and O_2-saturated 0.1 M KOH.

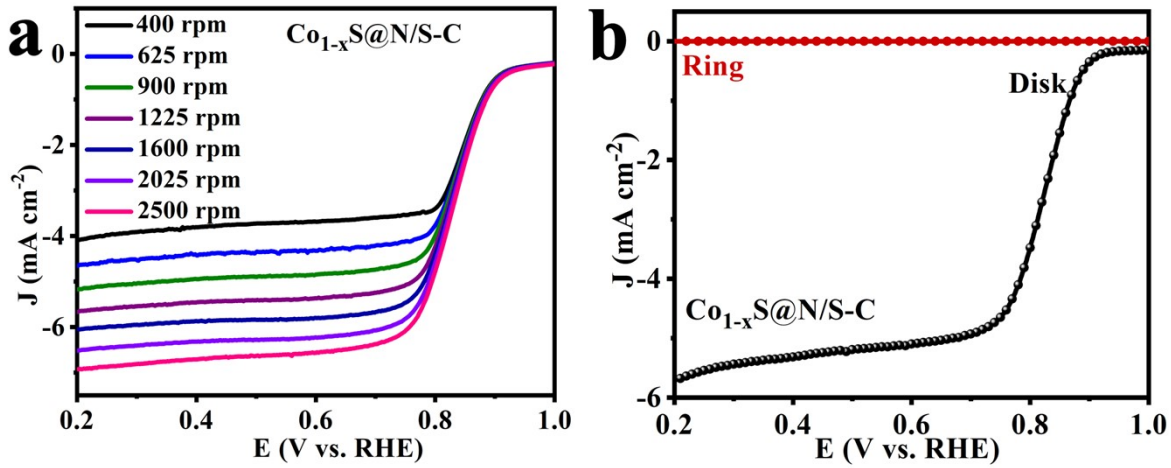

Figure S5. (a) LSV curves of the $Co_{1-x}S$@N/S-C catalyst at different rotating speeds from 400 to 2500 rpm and (b) The RRDE voltammograms of $Co_{1-x}S$@N/S-C at a rotating speed of 1600 rpm in O_2-saturated 0.1 M KOH.

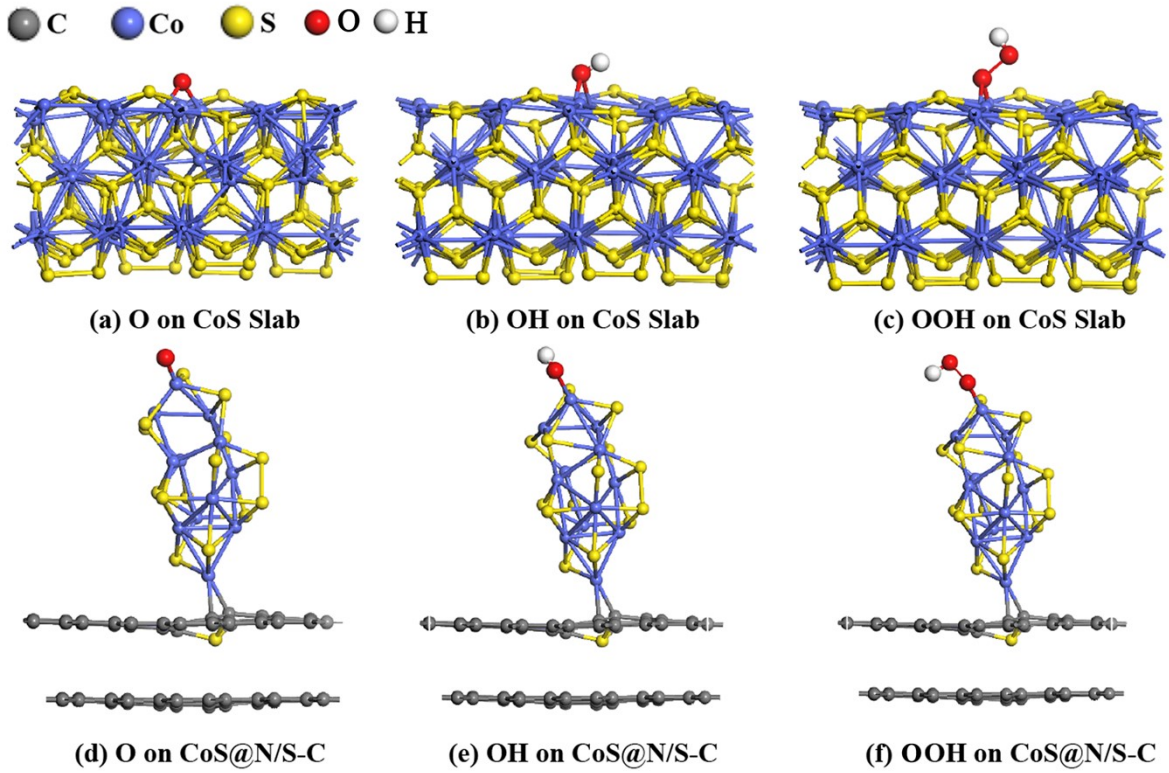

Figure S6. Optimized atomic configurations of oxygen intermediates (*O, *OH and *OOH) adsorbed on (a-c) CoS slab, (d-f) CoS@N/S-C models.

All the first-principles computations were carried out by employing the projector-augmented plane wave (PAW)[3,4] method as implemented in the Vienna *ab inito* simulation package (VASP)[5,6] code. The electron exchange-correlation functional was described by the generalized gradient approximation (GGA) in the form proposed by Perdew, Burke and

Ernzerhof (PBE).[7] The tolerance for energy convergence was set to 10^{-5} eV, while the ionic relaxation is converged when the force on each atom was less than 10^{-3} eV/Å. The 600 eV cutoff for plane-wave basis set was adopted in all computations. The Brillouin zone was integrated by using Monkhorst-Pack generated sets of *k*-points. In the geometry relaxation and self-consistent computations, 5×5×1 Monkhorst-Pack k-points mesh was used. The computational model of graphene consists of 144 carbon atoms arranged in honeycomb form, while the nitride/sulfide graphene has the carbon atoms replaced by N/S atoms. The CoS slab was cleaved to expose the (100) facet (Figure S6 a-c). The CoS clusters without and with Co vacancies was adsorbed on the bilayer N/S doped graphene, namely the CoS@N/S-C (Figure S6 d-f and Figure 5a). All the atomic configuration of oxygen intermediates adsorbed on different models are represented in Figure S6.

The Gibbs free energy for the catalytic steps in ORR and OER reactions was calculated by using the computational hydrogen electrode (CHE) method suggested by Nørskov and co-worker:[8]

$$G = E_{total} + ZPE - TS$$

The overall four-step OER pathways could be represented as

$* + H_2O(l) \rightarrow *OH + H^+ + e^-$

$*OH \rightarrow *O + H^+ + e^-$

$*O + H_2O \rightarrow *OOH + H^+ + e^-$

$*OOH \rightarrow * + O_2 + H^+ + e^-$

The ΔG values were calculated according to the Gibbs free energies of reaction status as listed above. For instance, the $\Delta G_I = G(*OH) + G(H) - G(*) - G(H_2O)$. The Gibbs free energies of H_2 and H_2O were calculated to be -6.89 and -14.35 eV, and the $G(O_2)$ were calculated according to the equation: $G(O_2) = 2\,G(H_2O) - 2\,G(H_2) + 4.92$ eV = -9.98 eV.

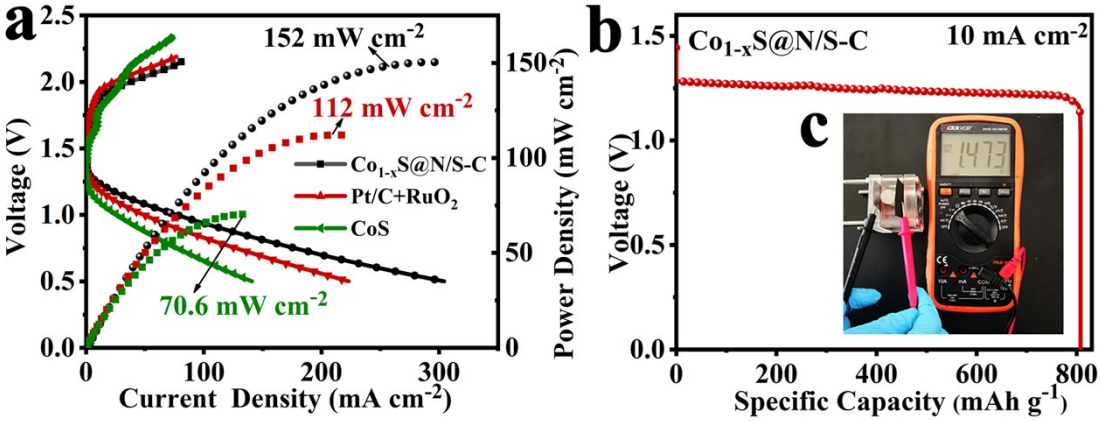

Figure S7. (a) Charge/discharge polarization curves and the power density curves of the liquid ZABs; (b) The specific capacity of $Co_{1-x}S$@N/S-C-based liquid ZAB under a constant current of 10 mA cm^{-2}; (c) Photograph of measured open-circuit potential for the $Co_{1-x}S$@N/S-C-based ZAB.

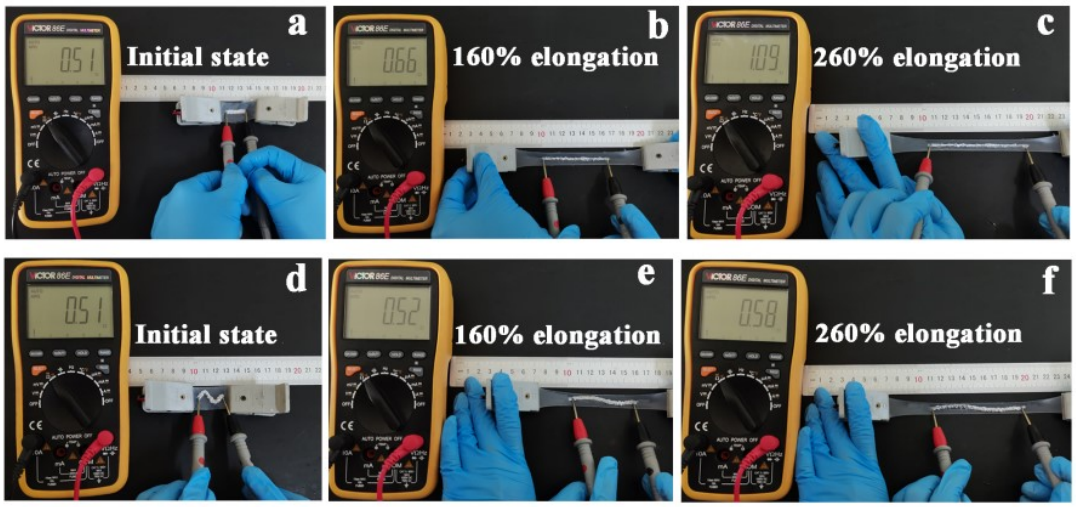

Figure S8. Optical images of the GaIn-Ni based electronic circuit adopted a linear configuration with a 2 mm line width under different deformation states: (a) 0% elongation, (b) 160% elongation, (c) 260% elongation; Optical images of the GaIn-Ni based electronic circuit adopted a wave-shaped configuration with a 2 mm line width under different deformation states: (d) 0% elongation, (e) 160% elongation, (f) 260% elongation.

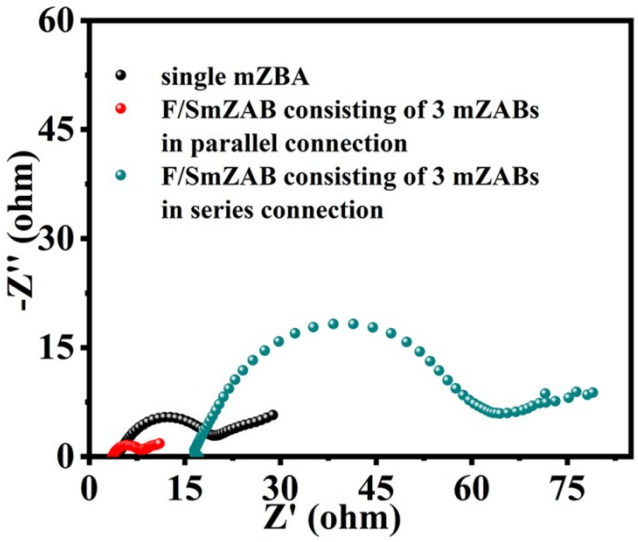

Figure S9. The EIS curves of the single $Co_{1-x}S$@N/S-C-based mZAB and the F/SmZAB with three integrated mZABs in series and parallel connection.

Table S1

Samples	Bond	CN	R (Å)	σ^2 (10^{-3} Å^2)	R-factor
CoS	Co-S	5.4±0.5	2.20±0.02	7.8±0.6	0.0003
$Co_{1-x}S$	Co-S	6.1±0.7	2.22±0.01	9.7±0.5	0.0004

Notes: Bond means the nearest and second nearest coordination shell. CN is coordination number, R is the bond length and σ^2 is Debye-Waller factor.

Table S2. Comparative summary of the cycling stability of liquid ZABs employing currently reported bifunctional electrocatalysts with our work.

Bifunctional electrocatalyst	Cycling stability of the liquid ZAB	Test conditions of liquid ZAB	Ref.
$Co_{1-x}S$@N/S-C	510 cycles (170 hours)	At a current density of 10 mA cm^{-2} (20 min per cycle) Electrolyte: 6 M KOH with 0.2 M zinc acetate solution	This work
Fe-Co_4N@N-C	220 cycles (36 hours)	At a current density of 5 mA cm^{-2} Electrolyte: 6 M KOH with 0.2 M zinc acetate solution	9
CoSx/Co-NC-800	450 cycles (90 hours)	At a current density of 5 mA cm^{-2} (12 min per cycle) Electrolyte: 6 M KOH with 0.2 M zinc acetate solution	10
Co@N-C	360 cycles (120 hours)	At a current density of 2 mA cm^{-2} (20 min per cycle) Electrolyte: 6 M KOH with 0.2 M zinc acetate solution	11
Co-N-C	120 cycles (60 hours)	At a current density of 20 mA cm^{-2} (30 min per cycle) Electrolyte: 6 M KOH with 0.2 M zinc acetate solution	12
COF_{BTC}	40cycles (80 hours)	At a current density of 10 mA cm^{-2} ((2 hours per cycle) Electrolyte: 8 M KOH with 0.5 M ZnO aqueous solution was used as the electrolyte	13
$Co_{5.47}N/Co_3Fe_7$/NC	180 h	At a current density of 10 mA cm^{-2} Electrolyte: 6 M KOH with 0.2 M zinc acetate solution	14
T-CoNCNTs // NiFe-LDH	100 cycles	At a current density of 50 mA cm^{-2} Electrolyte: 6 M KOH with 0.2 M zinc acetate solution	15
Mn-SAS/CN	25 hours	At a current density of 10 mA cm^{-2} Electrolyte: 6 M KOH with 0.2 M zinc acetate solution	16

References

1. J. Zhao, H. Hu and M. Wu, Nanoscale, 2020, 12, 3750-3762.

2. J. Zhao, H. Hu, W. Fang, Z. Bai, W. Zhang and M. Wu, J. Mater. Chem. A, 2021, 9, 5097-5110.

3. P. E. Blöchl, Phys. Rev. B, 1994, 50, 17953-17979.

4. D. Joubert, Phys. Rev. B - Condens. Matter Mater. Phys., 1999, 59, 1758-1775.

5. G. Kresse and J. Hafner, Phys. Rev. B, 1993, 48, 13115-13118.

6. R. A. Vargas-Hernández, J. Phys. Chem. A, 2020, 124, 4053-4061.

7. J. P. Perdew, K. Burke and M. Ernzerhof, Phys. Rev. Lett., 1996, 77, 3865-3868.

8. J. K. Nørskov, J. Rossmeisl, A. Logadottir, L. Lindqvist, J. R. Kitchin, T. Bligaard and H. Jónsson, J. Phys. Chem. B, 2004, 108, 17886–17892.

9. Q. Xu, H. Jiang, Y. Li, D. Liang, Y. Hu and C. Li, Appl. Catal. B Environ., 2019, 256, 117893.

10. Q. Lu, J. Yu, X. Zou, K. Liao, P. Tan, W. Zhou, M. Ni and Z. Shao, Adv. Funct. Mater., 2019, 29, 1904481.
11. M. Zhang, Q. Dai, H. Zheng, M. Chen and L. Dai, Adv. Mater., 2018, 30, 1705431.
12. H. Mei, M. Yang, Y. Shen, F. He, Z. Zhou, X. Chen, Y. Yang, S. Liu and Y. Zhang, Carbon N. Y., 2019, 144, 312-320.
13. P. Peng, L. Shi, F. Huo, S. Zhang, C. Mi, Y. Cheng and Z. Xiang, ACS Nano, 2019, 13, 878-884.
14. L. Li, J. Chen, S. Wang, Y. Huang and D. Cao, Appl. Surf. Sci., 2022, 582, 152375.
15. W. Xu, Z. Lu, T. Zhang, Y. Zhong, Y. Wu, G. Zhang, J. Liu, H. Wang and X. Sun, Energy Storage Mater., 2019, 17, 358-365.
16. X. Han, T. Zhang, W. Chen, B. Dong, G. Meng, L. Zheng, C. Yang, X. Sun, Z. Zhuang, D. Wang, A. Han and J. Liu, Adv. Energy Mater., 2021, 11, 2002753.